**Atmospheric
Chemistry
and Physics
Discussions**

This discussion paper is/has been under review for the journal *Atmospheric Chemistry and Physics (ACP)*. Please refer to the corresponding final paper in *ACP* if available.

First remote sensing measurements of ClOOCl along with ClO and ClONO$_2$ in activated and deactivated Arctic vortex conditions using new ClOOCl IR absorption cross sections

G. Wetzel[1], H. Oelhaf[1], O. Kirner[1], R. Ruhnke[1], F. Friedl-Vallon[1], A. Kleinert[1], G. Maucher[1], H. Fischer[1], M. Birk[2], G. Wagner[2], and A. Engel[3]

[1]Institut für Meteorologie und Klimaforschung (IMK), Karlsruhe Institute of Technology (KIT), Karlsruhe, Germany
[2]Deutsches Zentrum für Luft und Raumfahrt, Institut für Methodik der Fernerkundung, Wessling, Germany
[3]Institut für Atmosphäre und Umwelt, J. W. Goethe Universität Frankfurt, Frankfurt, Germany

Correspondence to: G. Wetzel (gerald.wetzel@kit.edu)

ACPD

9, 20103–20143, 2009

First remote sensing measurements of ClOOCl along with ClO and ClONO$_2$

G. Wetzel et al.

Title Page

Abstract | Introduction

Conclusions | References

Tables | Figures

|◄ | ►|

◄ | ►

Back | Close

Full Screen / Esc

Printer-friendly Version

Interactive Discussion

Abstract

Active chlorine species play a dominant role in the catalytic destruction of stratospheric ozone in the polar vortices during the late winter and early spring seasons. Recently, the correct understanding of the ClO dimer cycle was challenged by the release of new laboratory absorption cross sections (Pope et al., 2007) yielding significant model underestimates of observed ClO and ozone loss (von Hobe et al., 2007). Under this aspect, Arctic stratospheric limb emission measurements carried out by the balloon version of the Michelson Interferometer for Passive Atmospheric Sounding (MIPAS-B) from Kiruna (Sweden) on 11 January 2001 and 20/21 March 2003 have been reanalyzed with regard to the chlorine reservoir species ClONO$_2$ and the active species, ClO and ClOOCl (Cl$_2$O$_2$). New laboratory measurements of IR absorption cross sections of ClOOCl for various temperatures and pressures allowed for the first time the retrieval of ClOOCl mixing ratios from remote sensing measurements. High values of active chlorine (ClO$_x$) of roughly 2.3 ppbv at 20 km were observed by MIPAS-B in the cold mid-winter Arctic vortex on 11 January 2001. While nighttime ClOOCl shows enhanced values of nearly 1.1 ppbv at 20 km, ClONO$_2$ mixing ratios are less than 0.1 ppbv at this altitude. In contrast, high ClONO$_2$ mixing ratios of nearly 2.4 ppbv at 20 km have been observed in the late winter Arctic vortex on 20 March 2003. No significant ClO$_x$ amounts are detectable on this date since most of the active chlorine has already recovered to its main reservoir species ClONO$_2$. The observed values of ClO$_x$ and ClONO$_2$ are in line with the established chlorine chemistry. The thermal equilibrium constants between the dimer formation and its dissociation, as derived from the balloon measurements, are on the lower side of reported data and in good agreement with values recommended by von Hobe et al. (2007). Calculations with the ECHAM/MESSy Atmospheric Chemistry model (EMAC) using established kinetics show similar chlorine activation and deactivation, compared to the measurements in January 2001 and March 2003, respectively.

1 Introduction

Active ClO_x species ($Cl+ClO+2\,ClOOCl$) play an important role in the catalytic destruction of stratospheric ozone in the polar vortices during the late winter and early spring seasons after the release of chemically active chlorine compounds from the reservoir species HCl and $ClONO_2$ via heterogeneous chemical reactions. In the sunlit polar atmospheres, the ClO dimer cycle is one of the most important cycles for the destruction of polar ozone. The chlorine peroxide isomer ClOOCl (Cl_2O_2) is produced in the polar winter stratosphere when high ClO concentrations (0.5–2 ppbv) are available via the three body reaction (see, e.g. Brasseur and Solomon, 2005):

$$ClO + ClO + M \leftrightarrow ClOOCl + M \tag{R1}$$

Thereby, a thermal equilibrium K_{eq} between the dimer formation k_{rec} and dissociation k_{diss} according to (R1) exists:

$$K_{eq} = k_{rec}/k_{diss} = [ClOOCl]/[ClO]^2 \tag{1}$$

During daytime, the dimer is photolyzed:

$$ClOOCl + h\nu \rightarrow Cl + ClOO \tag{R2}$$

producing a chlorine atom and the ClOO radical which decomposes upon collision with an atmospheric molecule M (e.g. N_2 or O_2):

$$ClOO + M \rightarrow Cl + O_2 + M \tag{R3}$$

The Cl atom may react with ozone to produce chlorine monoxide again via:

$$Cl + O_3 \rightarrow ClO + O_2 \tag{R4}$$
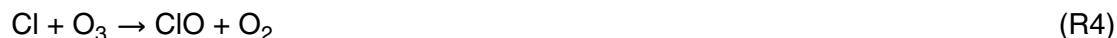
Taking into account twice Reaction (R4), the complete catalytic cycle leads to the following net reduction of ozone: $2\,O_3+h\nu\rightarrow 3\,O_2$. By the end of the Arctic winter, increasing amounts of NO_2 (produced mainly by HNO_3 photolysis) enhance the importance of the reaction:

$$ClO + NO_2 + M \rightarrow ClONO_2 + M \tag{R5}$$

Hence, active chlorine is transferred into ClONO$_2$, an important chemical reservoir species for chlorine.

Polar winter vertical profiles of ClONO$_2$ have been inferred from limb emission spectra measured by the balloon version of the Michelson Interferometer for Passive Atmospheric Sounding (MIPAS-B) for many years (see, e.g. von Clarmann et al., 1993; Oelhaf et al., 1994; von Clarmann et al., 1997; Stowasser et al., 2002; Wetzel et al., 2002, 2006). The high quality of the MIPAS-B ClONO$_2$ observations has been proven by comparisons to data of other instruments such as MIPAS on board the environmental satellite ENVISAT (Höpfner et al., 2004, 2007) and the first and second Improved Limb Atmospheric Spectrometer (ILAS) sensors (Nakajima et al., 2006; Wetzel et al., 2008) aboard the Japanese ADEOS satellites.

The radical ClO was retrieved for the first time from spectra measured by MIPAS-B during nighttime in February 1995 inside the Arctic vortex (von Clarmann et al., 1997). A ClO value of 0.4 ppbv near 16 km was inferred from the spectra. A daytime polar ClO climatology (1991–1998) was deduced from satellite observations of the Microwave Limb Sounder (MLS) on board the Upper Atmosphere Research Satellite (UARS; Santee et al., 2003). Arctic ClO values around 2 ppbv in the lower stratosphere were detected during time periods of chlorine activation. In the Antarctic, ClO values of nearly 3 ppbv have been observed by MLS. More recent ClO observations of comparable magnitude have been obtained by MLS on Aura at polar latitudes of both hemispheres between 2004 and 2006 (Santee et al., 2008). ClO mixing ratios of up to 2.5 ppbv during day and up to 0.5 ppbv during night have been measured inside the lower stratospheric Antarctic vortex in September and October 2002 by MIPAS on ENVISAT (Glatthor et al., 2004).

The isomer ClOOCl has been observed in the Arctic stratosphere in winter 1999/2000 aboard a NASA ER-2 aircraft, deployed from Kiruna, Sweden (Stimpfle et al., 2004). Besides ClONO$_2$ and ClO, ClOOCl was detected in-situ by thermal dissociation into two ClO fragments that are measured by a chemical conversion technique. Nighttime ClOOCl values of up to 1.1 ppbv with an accuracy of 21% were observed on

2 February 2000 near 20 km inside the polar vortex. Daytime in-situ ClOOCl values of up to 0.2 ppbv were observed by the HALOX instrument aboard the M55-Geophysica aircraft inside the Arctic vortex on 7 March 2005 (von Hobe et al., 2007).

Recently, the correct understanding of the ClO dimer cycle was challenged by the release of new laboratory absorption cross sections (Pope et al., 2007) yielding to significant model underestimates of observed ClO and ozone loss (von Hobe et al., 2007). Under this aspect, nighttime Arctic stratospheric limb emission measurements carried out by MIPAS-B from Kiruna, Sweden on 11 January 2001 and 20/21 March 2003 have been reanalyzed with regard to the chlorine reservoir species $ClONO_2$ and the active ClO_x species ClO and, for the first time, ClOOCl. To our knowledge, these measurements constitute the first simultaneous observations of ClO, ClOOCl and $ClONO_2$ over extended altitude regions in the lower stratosphere. Retrieved trace gas profiles are used to derive ClO/ClOOCl equilibrium constants and are compared to 3-dimensional chemical modelling.

2   MIPAS-B instrument and flight situations

The balloon-borne cryogenic Fourier transform spectrometer MIPAS-B is a limb-emission sounder which covers the mid-infrared spectral range from 4 to 14 µm. Besides a high performance and flexibility of the pointing system with a knowledge of the tangent altitude of better than 50 m at the 1-σ confidence limit, MIPAS-B spectra are characterized by their high spectral resolution (about 0.07 cm^{-1} after apodization) allowing the separation of individual spectral lines from continuum-like emissions in combination with a high radiometric accuracy. Typical values of the noise equivalent spectral radiance (NESR) are within 10^{-9} and 10^{-8} W/(cm^2 sr cm^{-1}) for a single calibrated spectrum leading to signal-to-noise values of several hundreds in case of the prominent spectral features. A comprehensive overview and description of the instrument is given by Friedl-Vallon et al. (2004) and references therein. It includes instrument characterization in terms of the instrumental line shape, field of view, noise equivalent

Full Screen / Esc

Printer-friendly Version

Interactive Discussion

spectral radiance, line of sight of the instrument, detector nonlinearity and the error budget of the calibrated spectra.

Arctic winter MIPAS-B flights in 2001 and 2003 were carried out from Kiruna (Sweden, 68° N, 21° E). The first one was performed in the night on 11 January 2001 inside a cold polar vortex with synoptic polar stratospheric clouds (PSCs; Höpfner et al., 2002). This winter was characterized by a variety of dynamical changes in the northern hemisphere (European Ozone Research Coordinating Unit, 2001). The usual seasonal cooling in the polar region and the strengthening of the Arctic vortex was interrupted in the second half of November by a strong Canadian warming in the lower stratosphere. After the weakening of this warming in the beginning of December, a strong upper stratospheric warming developed. From late December to mid-January, the period where the MIPAS-B flight took place, the vortex strengthened and cooled again such that temperatures fell below the PSC existence threshold temperature for the nucleation of nitric acid trihydrate particles (T_{NAT}) at 30 hPa ($\sim$22 km) and below. MIPAS-B spectra of the southward scan (performed outside of PSCs) were recorded from a float altitude of 28.1 km during nighttime between 15:16 UTC and 15:58 UTC covering 14 limb scans from +2° to −4.2° elevation angles corresponding to a lowermost tangent altitude of 10.4 km. The coordinates of the mean tangent points are 65.2° N, 33.5° E, corresponding to a measurement clearly inside the polar vortex (see Fig. 1).

An overview on the meteorological situation in the winter 2002/03 is given by the European Ozone Research Coordinating Unit (2003) and Grooß et al. (2005). This winter started with low stratospheric temperatures below T_{NAT}. A major warming in mid-January was followed by a re-formation of the vortex which was split by a minor warming around mid-February. The vortex was re-established by the beginning of March, again with temperatures below the threshold for PSC formation in its cold centre above Scandinavia, but only for a couple of days. The MIPAS-B observations were performed in the night from 20–21 March 2003. During this time the vortex was slightly warmed-up but still stable because its centre was tightly coupled to the cold centre in the lower stratosphere. Several limb scans could be recorded during this long

Title Page

Abstract | Introduction

Conclusions | References

Tables | Figures

|◄ | ►|

◄ | ►

Back | Close

Full Screen / Esc

Printer-friendly Version

Interactive Discussion

lasting flight from 18:22 UTC (20 March) to 09:38 UTC (21 March) including continuous observations before, during, and after sunrise illustrating the evolution of photochemically active gases like NO_2 and N_2O_5 (Wiegele et al., 2009). Spectra of the fourth (nighttime) sequence measured between 21:39 UTC and 22:18 UTC from a float altitude of 31.0 km have been used for this study. Seventeen limb scans from $+2°$ to $-4.7°$ elevation angles corresponding to a lowermost tangent altitude of 8.8 km (mean tangent point coordinates: 65.6° N, 27.2° E) were recorded inside the polar vortex in the absence of PSCs (see Fig. 1).

3 Radiance sensitivity studies using new ClOOCl IR cross sections

Radiance simulations were performed to assess, in terms of detectability and random and systematic errors, the principal potential of MIPAS-B to measure chlorine species like ClO and ClOOCl which are, in contrast to $ClONO_2$, not easily detectable. Limb emission radiances were calculated with the KOPRA (Karlsruhe Optimized and Precise Radiative transfer Algorithm) radiative transfer model (Stiller et al., 2002). Spectroscopic parameters for the calculation of limb emission spectra were taken from the HITRAN database (Rothman et al., 2005). Line data of ClO originate from spectroscopic measurements carried out by Burkholder et al. (1989) and Goldman et al. (1994). Cross sections for $ClONO_2$ have been measured by Wagner and Birk (2003).

3.1 ClOOCl IR cross sections

ClOOCl cross sections in the IR spectral domain used for the retrieval of ClOOCl mixing ratios have been determined within the same project as $ClONO_2$, funded by the German "Ozon-Forschungsprogramm" (Wagner and Birk, 2001). For ClOOCl, this work is discussed in the following section.

ClOOCl was produced in a flow reactor from atomic chlorine (Cl_2 flow through microwave discharge) and Cl_2O (Cl_2 flow through yellow mercury oxide, HgO) forming

Title Page

Abstract | Introduction

Conclusions | References

Tables | Figures

|◄ | ►|

◄ | ►

Back | Close

Full Screen / Esc

Printer-friendly Version

Interactive Discussion

ClO and subsequent dimerization at low temperatures (Birk et al., 1989). The flow reactor was attached to a coolable multireflection cell set to a 59.2 m absorption path. The residence time in the cell was about 50 s corresponding to a volume flow of ca. 0.5 l/s. In order to suppress bimolecular conversion of ClO into Cl_2 and O_2, as well as OClO and Cl_2O_3 formation, the gas flows (Cl in He and Cl_2O in He/N_2) were cooled below 210 K shortly after mixing, before injection into the multireflection cell. Furthermore, one measurement was attributed to investigate the yield of ClOOCl from ClO. In order to suppress the ClOOCl decomposition by the reaction $ClOOCl+Cl \rightarrow Cl_2+O_2+Cl$, a large excess of Cl_2O was used (probability of ClOOCl destruction is proportional to the number density ratio of $ClOOCl/Cl_2O$). The flow conditions were held stable for some hours allowing for subsequent low resolution mid infrared (MIR, 500–800 cm^{-1}), far infrared (FIR, 15–25 cm^{-1}) and again a low resolution mid infrared measurement. The low resolution measurements were used to scale absorption cross sections from high resolution mid infrared spectra (0.0028 cm^{-1} for 20 hPa measurements, 0.0056 cm^{-1} for 40 hPa measurements). Furthermore, the low resolution MIR measurements served as an indicator that the conditions have indeed been stable. All measurements were carried out with a Bruker IFS 120 HR; the coolable multireflection cell was developed at the German Aerospace Centre (DLR). The far infrared measurements were used for calculating the number densities needed for calculation of the mid infrared absorption cross sections. Line strengths for the pure rotational far infrared transitions were derived from the JPL line catalogue (Pickett et al., 1998). The JPL data were calculated from the permanent electric dipole moment. Furthermore, the vibrational partition function was calculated since this is not included in the JPL catalogue, using the following fundamental wavenumbers: 127.0, 328.0, 443.0, 560.0, 653.0, and 752.0 cm^{-1}. Since the FIR spectra contained lines outside the quantum number range of previous work (Birk et al., 1989) quantum mechanical fits with the JPL software CALFIT were performed yielding refined centrifugal distortion parameters. The program CALCAT was then used for improved frequency predictions taken as input in the line fitting software FITMAS (Wagner et al., 2002). FITMAS resulted in scaled line strengths for individual

rotational transitions for both the $^{35}ClOO^{35}Cl$ and $^{35}ClOO^{37}Cl$ isotopologues each in the ground and first excited torsional state. Figure 2 shows an example of one microwindow region of the FIR spectrum together with the modelled spectrum from the line fitting. From the scaled line strength data (ca. 400 lines in the ground- and ca. 200 in the torsionally excited state) and the JPL catalogue line strengths considering vibrational partitioning, number densities and the average gas temperature could be fitted.

The largest uncertainty in the reference line strengths is caused by the large uncertainty in the torsional wavenumber ($127\pm20\,cm^{-1}$) from previous work (Birk et al., 1989). Its fundamental wavenumber could be refined from relative intensities of rotational transitions in the ground and torsionally excited states to $111.5\pm8.5\,cm^{-1}$. Average number densities of about 10^{15} molecules cm^{-3} were achieved. The number density uncertainty is 10% calculated by the root sum square of the following uncertainty contributions: 2% from permanent electric dipole moment uncertainty, 5% from uncertainty in vibrational partition sum, 7% from temperature error, and 4% statistical error from number density fitting.

When calculating the number density from the titrated amount of the precursor Cl_2O a 20% higher value was found. This shows that the ClO self reaction indeed produces almost only ClOOCl and is also a proof for the average number density determination. It should be noted that the number density determination from the FIR is highly specific since it was fitted together with the gas temperature from 400 individual rotational transitions. Another important question should be addressed: Is the number density in the FIR path the same as for the MIR path? Due to the nature of the flow experiment the ClOOCl distribution in the cell may not be homogeneous. In the present experiment, exactly the same optics was used for the FIR and MIR experiments except for the beamsplitter, detector, and entrance aperture size. Thus the optical path is nearly identical.

Finally, four sets of absorption cross sections were obtained for combinations of temperatures 225 K and 250 K and total pressures 20 hPa and 40 hPa in the range

Title Page

Abstract | Introduction

Conclusions | References

Tables | Figures

|◄ | ►|

◄ | ►

Back | Close

Full Screen / Esc

Printer-friendly Version

Interactive Discussion

500–800 cm^{-1} covering the 3 fundamentals with different integrated band strengths: v_2 (Cl–O symmetric stretch, 510–600 cm^{-1}, 2.16×10^{-18} cm^{-1} cm^2 molecule^{-1}), v_5 (Cl–O asymmetric stretch, 620–680 cm^{-1}, 3.07×10^{-18} cm^{-1} cm^2 molecule^{-1}), and v_1 (O–O stretch, 710–790 cm^{-1}, 9.35×10^{-19} cm^{-1} cm^2 molecule^{-1}). The total uncer-
tainty of the absorption cross sections is 12%. Figure 3 shows the absorption cross section for the v_1 band relevant for the present paper. The strongest band v_5 is blended by CO_2, the second strongest band v_2 lies outside the spectral range of MIPAS-B, thus the weakest band was used.

The only published mid infrared band intensity results by Brust et al. (1997) are a fac-
tor of 3 smaller. They used parallel UV measurements for number density determina-
tion. According to Pope et al. (2007) the UV cross section data are accurate enough for number density determination with 10% accuracy. The factor of 3 discrepancy may be caused by the different UV and mid infrared optical path through the highly inhomo-
geneous ClOOCl sample in the flow setup. As already mentioned, in the present work the optical path for FIR and MIR was almost identical. Assuming that the absorption cross sections of Brust et al. (1997) are correct, this would imply that our number den-
sity should be 3 times larger than our actual result. This is impossible since for 100% conversion the ClOOCl amount can only be 20% larger.

3.2 Radiance sensitivity calculations

Radiance sensitivities to changes in the mass of the species ClO, ClOOCl, and ClONO$_2$ have been computed in selected spectral regions (see Table 1). Radiance calculations are based on Arctic winter profiles of stratospheric species and temperature, selected for typical cases of activated and deactivated stratospheric conditions at day and night inside the polar vortex. Vertical profiles of the chlorine species used for the sensitivity calculations are shown in Fig. 4. ClO and ClOOCl represent situations of activated chlorine for day and night conditions, respectively. Daytime ClOOCl values are very small and therefore not detectable with MIPAS-B. The diurnal variation of ClONO$_2$ can

First remote sensing measurements of ClOOCl along with ClO and ClONO$_2$

G. Wetzel et al.

be neglected. This profile stands for a situation at the end of the polar winter where active chlorine has already been converted to this reservoir species. Assuming a float altitude of 31 km, a total of 12 limb scans down to 13.5 km with a vertical spacing of 1.5 km have been simulated, representing a typical MIPAS-B measurement scenario in the Arctic. The following kinds of simulations were performed in order to assess the principal detectability of the target species given the NESR of MIPAS-B: Based on the reference run with the standard atmosphere, the mass m of the target molecule was either enhanced by 20% or set to zero (−100%). From the changing radiance signal the radiance difference (ΔL) to the reference run can be calculated at each spectral grid point i and further on be divided by the MIPAS-B noise equivalent spectral radiance (*NESR*) of the MIPAS-B instrument:

$$SNR_i = \frac{\Delta L_i(\Delta m)}{NESR_i} \qquad (2)$$

where SNR_i is the signal to noise ratio at each spectral grid point. Taking into account many independent spectral grid points N with radiance contributions of the target molecule improves the signal to noise ratio:

$$SNR_N = \frac{1}{\sqrt{N}} \sum_{i=1}^{N} \frac{\Delta L_i(\Delta m)}{NESR_i} \qquad (3)$$

where SNR_N refers to a spectral interval.

Results of the radiance simulations are compiled in Table 1. ClO calculations were carried out in the P-branch region of the 11.8 µm band which is characterized by comparatively little interference with other species. A spectral window containing a well-separated ClO signature is displayed in Figs. 5 and 6. The main interfering species in this microwindow is the molecule O$_3$. A significant difference is visible in the strength of the ClO signature between day (Fig. 5) and night (Fig. 6) conditions. While during day, a 20% change in the mixing ratio of ClO yields to a signal to noise ratio of 4.4 (see Table 1), the nighttime signal to noise ratios are less than unity such that noise errors of

more than 20% can be expected when this species is derived from nocturnal MIPAS-B spectra.

Radiance calculations in the spectral region of the ClOOCl band centred near $753\,cm^{-1}$ are shown in Fig. 7. The spectrum is dominated by contributions of the molecules O_3 and CO_2. The maximum difference between the radiance calculated with elevated nighttime ClOOCl and without ClOOCl (what corresponds to daytime conditions) is about two times the spectral noise of the MIPAS-B instrument for a single spectral grid point. Taking into account a large number of independent grid points in this wide spectral window will significantly improve the signal to noise ratio (see Table 1) according to Eq. (3). Hence, high values of ClOOCl should be detectable with MIPAS-B. However, it must be mentioned that interferences with other species are strong, especially in the P-branch region of the ClOOCl band below $750\,cm^{-1}$. Systematic errors are therefore expected to play an important role during the retrieval process of the target molecule ClOOCl (see Sect. 4).

Radiance simulations of the species $ClONO_2$ are depicted in Fig. 8. The $ClONO_2$ Q-branch at $780.2\,cm^{-1}$ shows up as a strong signature between two adjacent O_3 lines. Signal to noise ratios are large (see Table 1); consequently, noise errors during the retrieval are expected to be small (see Sect. 4).

4   Retrieval results and model comparison

In this section, retrieved profiles of the chlorine species ClO, ClOOCl, and $ClONO_2$, are discussed and compared to simulations performed with a chemical model.

Retrieval calculations were carried out with a least squares fitting procedure using analytical derivative spectra calculated by KOPRA (Höpfner et al., 2002). While the vertical distance of the observed tangent altitudes amounts between 0.8 and 1.7 km, the retrieval grid was set to 1 km up to the balloon float altitude, whereas above, the vertical spacing slightly increases to 10 km at 100 km altitude. A Tikhonov-Phillips regularization approach was applied which was constrained with respect to a height-

constant zero a priori profile of the target species. The number of degrees of freedom of the retrieval, which corresponds to the trace of the averaging kernel matrix, is listed in Table 1. A large number of degrees of freedom corresponds with a high altitude resolution (and vice versa) as in the case of $ClONO_2$ where 1.5–3 km (dependent on altitude) are reached since there is much information on the vertical distribution of this species contained in the measured spectra of the limb sequence. In contrast, the altitude resolution is limited to 3–7 km in the case of ClO and ClOOCl. All chlorine species have been analyzed in the spectral windows which are listed, together with interfering species, in Table 1. Concerning ClOOCl, only the R-branch part of the 13.3 µm band above 755 cm^{-1} has been used for the retrieval calculations because the P-branch region was not available due to the special optical filter configuration during the January 2001 flight. Besides temperature, prominent interfering gases were adjusted simultaneously together with the target molecule, frequency shift, and radiance offset. Less prominent interfering species were previously fitted in appropriate spectral regions.

A best fit in the spectral region of the molecule ClOOCl is shown in Fig. 9. Main interfering species are O_3, CO_2, HNO_3, and $ClONO_2$. Mean deviations in the residual spectra are close to the noise level of the measured spectra. Features in the residual spectra deviating from white noise are mostly connected with strong and dense transitions of the molecules O_3 and CO_2 as, e.g., near 758, 763, and 771 cm^{-1}, most probably caused by spectroscopic inaccuracies and line mixing effects. However, the information on the amount of ClOOCl is contained in the gradually changing shape of the emission of its R-branch along the frequency scale. This is reflected by the difference of the retrievals performed with and without the species ClOOCl (green solid line in Fig. 9). Introducing the (small) emission of ClOOCl into the retrieval slightly improves the root of mean squares of the residual which is dominated by the imperfect fitting of the prominent CO_2 and O_3 features.

The error estimation consists of random and systematic errors. Random errors include spectral noise as well as covariance effects of the fitted parameters. Systematic errors mainly comprise spectroscopic data errors (band intensities), uncertainties in

Title Page

Abstract | Introduction

Conclusions | References

Tables | Figures

◄◄ | ►►

◄ | ►

Back | Close

Full Screen / Esc

Printer-friendly Version

Interactive Discussion

the line of sight, and CO_2 line mixing effects. Errors of the non-simultaneously fitted interfering gases were estimated with test retrievals and also treated as systematic. Random and systematic errors were added quadratically to yield the total error which refers to the 1-σ confidence limit.

Retrieved volume mixing ratios for the January 2001 flight are depicted in Fig. 10 together with their random and total errors. As expected from the large signal to noise ratio (cf. Sect. 3), the $ClONO_2$ random error is very small, except at 20 km, where the mixing ratio is close to zero. The total error, which is dominated by the spectroscopic data uncertainty (5% in band intensity), is close to 5% in regions where $ClONO_2$ mixing ratios are larger than 0.3 ppbv. Concerning the molecule ClO, random noise is the dominating error source since nighttime ClO mixing ratios are small and hence the signal to noise ratio is as well (cf. Sect. 3). In contrast, the large number of spectral grid points is reducing the noise error for the species ClOOCl. Here, systematic error sources are also relevant. Besides spectroscopy (band intensity error: 12%), uncertainties due to interfering gases and, to a lesser extent, line of sight errors, dominate this kind of error. Above 22 km and below 19 km, no ClOOCl mixing ratios could be retrieved since the amounts of ClOOCl are below the detection limit which is several tenths of ppbv.

Retrieved profiles of the chlorine species $ClONO_2$, ClO, and ClOOCl, as measured by MIPAS-B during the mid-winter flight on 11 January 2001 and the late winter flight on 20 March 2003 inside the polar vortices are displayed in Figs. 11 and 12.

To obtain a proxy of total inorganic chlorine Cl_y a N_2O-Cl_y correlation was derived from measurements performed on air samples collected with the balloon-borne cryogenic whole air sampler BONBON in the Arctic winters between the years 2000 and 2003 (Engel et al., 2006). This correlation has been deduced taking into account in-situ N_2O and chlorine measurements of CFC-11, CFC-12, CFC-22, CFC-113, CCl_4, CH_3CCl_3, and CH_3Cl. The organic chlorine determined as the sum of these species was increased by 3% in order to account for long lived chlorine source gases which were not measured on these samples, in particular HCFC-141b and HCFC-142b. Cl_y

is then calculated as the difference between the organic chlorine determined in this way and the total chlorine calculated from the tropospheric burden of chlorine source gases taking into account the mean age of the air (Engel et al., 2002). Data for chlorine source gases are taken from NOAA ESRL GMD (National Oceanic and Atmospheric Administration, Earth System Research Laboratory, Global Monitoring Division; Montzka et al., 1999). 150 pptv of chlorine were added to account for very short lived species (VSLS) and unmeasured chlorine source gases. A polynomial fit was applied to calculate the proxy inorganic chlorine [Cl_y^*] calculated in this way in dependence of [N_2O], both given in ppbv:

$$[Cl_y^*] = 3.4954 - 1.3849 \times 10^{-3}[N_2O] - 1.9941 \times 10^{-5}[N_2O]^2 - 3.2180 \times 10^{-8}[N_2O]^3 . \quad (4)$$

This correlation has been adapted to MIPAS-B measured N_2O and yields up to 3.5 ppbv Cl_y^* in the stratosphere. Cl_y^* differences between 18 and 25 km reflect the stronger subsidence of air masses in late winter 2003 compared to the case in earlier winter 2001. The amount of residual inorganic species [$Cl_{y res}^*$]=[HCl]+[HOCl]+[. . .] which are not directly measured can be calculated via:

$$[Cl_{y\ res}^*] = [Cl_y^*] - [ClO_x] - [ClONO_2] . \quad (5)$$

The nighttime MIPAS-B observations in January 2001, which were carried out about 2.5 h after local sunset, show enhanced ClOOCl values with a maximum mixing ratio of nearly 1.1 ppbv at 20 km altitude. As expected, low nocturnal ClO values below 0.3 ppbv were detected all over the lower stratosphere. ClO_x shows a peak value of about 2.3 ppbv at 20 km. This layer of activated chlorine is reflected by very low mixing ratios of the chlorine reservoir species $ClONO_2$ with values of less than 0.1 ppbv at 20 km altitude and reduced mixing ratios of $Cl_{y\ res}^*$ which consists mainly of HCl.

In contrast to the mid-winter January 2001 situation, the nocturnal observations carried out in March 2003 exhibit very high $ClONO_2$ values (nearly 2.4 ppbv at 20 km) which are typical for the late winter Arctic vortex when active chlorine has been converted to this reservoir species via Reaction (R5). This $ClONO_2$ profile, together with

further profiles of nitrogen species and tracers like N_2O and CH_4, has already been discussed by Wetzel et al. (2008). Such high $ClONO_2$ amounts have also been measured in earlier late winter vortices by MIPAS-B (von Clarmann et al., 1993; Oelhaf et al., 1994; Wetzel et al., 2002). An activated chlorine layer is not visible in these measurements. No significant ClOOCl values could be retrieved. Inferred ClO_x values are also close to zero.

Measured profiles are compared to calculations performed with the Chemistry Climate Model (CCM) EMAC (ECHAM/MESSy Atmospheric Chemistry model) developed at the Max-Planck-Institute for Chemistry in Mainz (Jöckel et al., 2006). EMAC is a combination of the general circulation model ECHAM5 (Roeckner et al., 2006) and different submodels as, for instance, the chemistry submodel MECCA (Sander et al., 2005) combined through the interface Modular Earth Submodel System (MESSy; Jöckel et al., 2005).

For this study data from a nine year simulation from 2000 to 2008 with EMAC Version 1.7 are used. The simulation was performed with horizontal resolution T42 ($2.8°\times2.8°$) and with 39 layers, covering the atmosphere from the surface up to 0.01 hPa (approx. 80 km). A Newtonian relaxation technique of the prognostic variables temperature, vorticity, divergence and the surface pressure above the boundary layer and below 10 hPa towards ECMWF operational analysis data has been applied, in order to nudge the model dynamics towards the observed meteorology. The boundary conditions for greenhouse gases are from the IPCC-A1B scenario (IPCC, 2001) adapted to observations from the AGAGE database (Prinn et al., 2001) and for halogenated hydrocarbons from the WMO-Ab scenario (WMO, 2007). The simulation includes a comprehensive atmospheric chemistry setup for the troposphere, the stratosphere and the lower mesosphere. Rate constants of gas-phase reactions and surface reaction probabilities are mainly taken from the compilation by Sander et al. (2003). This holds also for the ClOOCl dimer dissociation Reaction (R1) and the absorption cross section photolysis Reaction (R2). The ClOOCl recombination is calculated according to the International Union of Pure and Applied Chemistry (IUPAC) recommendation (Atkinson et al., 2007).

◄◄ | ►►

◄ | ►

Back | Close

Full Screen / Esc

Printer-friendly Version

Interactive Discussion

The applied submodels are the same as in the simulations in Kirner (2008). In particular we used a new parameterisation of polar stratospheric clouds based on the efficient growth and sedimentation of NAT-particles in the submodel PSC (Kirner, 2008).

A comparison of measured and simulated chlorine species for both discussed winter situations is shown in Figs. 13 and 14. To separate dynamical from chemical effects, ratios of individual Cl_y components to total inorganic chlorine are calculated here. The chlorine activation (ClO_x/Cl_y^*) as measured by MIPAS-B in January 2001 (Fig. 13) is quite well reproduced by the EMAC model where the altitude region of the activation is slightly broader compared to the observation, with an extension to lower altitudes. This can be explained by the history of the PSC particles in the model which fell down in the course of the cold winter to altitudes below 19 km and which consequently caused chlorine activation in the model. The EMAC model is also able to reproduce measured $ClONO_2/Cl_y^*$ and $C_{y\,res}^*/Cl_y^*$ ratios in a consistent manner.

In March 2003, no chlorine activation was measured in the lower stratosphere. This is also displayed by the EMAC simulations. Observed $ClONO_2/Cl_y^*$ and $Cl_{y\,res}^*/Cl_y^*$ ratios are again well reproduced by the model simulations.

Figure 15 depicts K_{eq} values as deduced from MIPAS-B observations on 11 January 2001 and EMAC simulations according to Eq. (1). Measured and modelled K_{eq} values lie close together. On the other hand, data from the literature (see, von Hobe et al., 2007, and references therein) span a wide region of equilibrium constants in the lower stratosphere. MIPAS-B and EMAC values are located in the lower part of the shaded region in Fig. 15. This is in good agreement with equilibrium constants inferred by von Hobe et al. (2005) and Plenge et al. (2005) which were recommended by von Hobe et al. (2007).

5   Conclusions

Nighttime Arctic stratospheric limb emission measurements were carried out by MIPAS-B from Kiruna, Sweden on 11 January 2001 and 20/21 March 2003 inside the polar vor-

tices under activated and deactivated chlorine (ClO$_x$) conditions. The winter 2000/2001 was characterized by a very cold period in the lower stratosphere before and during the time of the MIPAS-B flight. Polar stratospheric clouds could form since the end of December when temperatures sank below T_{NAT} in the lower stratosphere. Hence,
5   activation of chlorine (ClO$_x$) was possible via heterogeneous chemistry on cloud particles right before the MIPAS-B flight. Measured spectra were analyzed with regard to the chlorine reservoir species ClONO$_2$ and the active ClO$_x$ species, ClO and ClOOCl. Significant amounts of nighttime ClOOCl (nearly 1.1 ppbv at 20 km) could be observed by MIPAS-B for the first time in an altitude region where an enhanced value is ex-
10   pected to occur. The amount of observed ClOOCl (using our new cross sections) is in agreement with nighttime Arctic vortex ClOOCl mixing ratios measured in-situ in February of the previous winter in the same altitude region (Stimpfle et al., 2004). It is worth mentioning that if the Brust et al. (1997) ClOOCl cross sections were used for the analysis, our retrieved ClOOCl mixing ratios would be enhanced by a factor of 3
15   leading to unreasonably high values of more than 3 ppbv for this species (and accordingly more than 6 ppbv Cl$_y$). Radiance sensitivity calculations have underpinned the feasibility of measuring ClOOCl under chlorine activated conditions by taking into account a large number of spectral grid points. Low values of nocturnal ClO (0.2 ppbv at 20 km) and very low ClONO$_2$ mixing ratios of less than 0.1 ppbv reveal a consistent pic-
20   ture of the chlorine partitioning observed during this flight which can be expected from the established chlorine chemistry. During the time of the MIPAS-B observation inside the late March 2003 polar vortex the situation was very different. ClO$_x$ had already dropped to values close to zero, which are typical for normal non-activated gas-phase conditions. No significant ClOOCl data could be retrieved from the recorded spectra.
25   Accordingly, the chlorine reservoir species ClONO$_2$ reached very high values of up to 2.4 ppbv at 20 km. Simulations with the CCM EMAC show that the model is able to reproduce the observed activated and deactivated chlorine conditions quite well using established kinetics.

Altogether we conclude that the first simultaneous atmospheric remote sensing mea-

surements of ClO, ClOOCl and ClONO$_2$ at different geophysical conditions in the polar stratosphere are in line with the established chlorine chemistry. This also holds for the derived MIPAS-B ClO/ClOOCl equilibrium constant K_{eq} which has been compared to literature data calculated using MIPAS-B temperatures (range: 192–203 K). EMAC K_{eq}
5 data are in line with MIPAS-B results and both K_{eq} data are characterized by comparatively smaller values (less than 2×10^{-8} molecules cm^{-3}) supporting the findings of von Hobe et al. (2007).

References

Atkinson, R., Baulch, D. L., Cox, R. A., Crowley, J. N., Hampson, R. F., Hynes, R. G.,
15   Jenkin, M. E., Rossi, M. J., and Troe, J.: Evaluated kinetic and photochemical data for atmospheric chemistry: Volume III – gas phase reactions of inorganic halogens, Atmos. Chem. Phys., 7, 981–1191, 2007,
http://www.atmos-chem-phys.net/7/981/2007/.
Birk, M., Friedl, R. R., Cohen, E. A., and Pickett, H. M.: The rotational spectrum of chlorine
20   peroxide, J. Chem. Phys., 91, 6588–6597, 1989.
Brasseur, G. and Solomon, S.: Aeronomy of the middle atmosphere (third edition), Springer, Dordrecht, 369 pp., 2005.
Brust, A. S., Zabel, F., and Becker, K. H.: Integrated IR band intensities of the v_5 and v_1 bands of ClOOCl, Geophys. Res. Lett., 24, 1395–1398, 1997.
25 Burkholder, J. B., Hammer, P. D., Howard, C. J., and Goldman, A.: Infrared line intensity measurements in the v=0–1 band of the ClO radical, J. Geophys. Res., 94, 2225–2234, 1989.
Engel, A., Strunk, M., Müller, M., Haase, H.-P., Poss, C., Levin, I., and Schmidt, U.: Temporal development of total chlorine in the high-latitude stratosphere based on reference

Title Page

Abstract | Introduction

Conclusions | References

Tables | Figures

◄◄ | ►►

◄ | ►

Back | Close

Full Screen / Esc

Printer-friendly Version

Interactive Discussion

distributions of mean age derived from CO_2 and SF_6, J. Geophys. Res., 107(D12), 4136, doi:10.1029/2001JD000584, 2002.

Engel, A., Möbius, T., Haase, H.-P., Bönisch, H., Wetter, T., Schmidt, U., Levin, I., Reddmann, T., Oelhaf, H., Wetzel, G., Grunow, K., Huret, N., and Pirre, M.: Observation of mesospheric air inside the arctic stratospheric polar vortex in early 2003, Atmos. Chem. Phys., 6, 267–282, 2006,
http://www.atmos-chem-phys.net/6/267/2006/.

European Ozone Research Coordinating Unit: The Northern Hemisphere stratosphere in the 2000/01 winter, http://www.ozone-sec.ch.cam.ac.uk/EORCU/reports/wr0001t.pdf, 2001.

European Ozone Research Coordinating Unit: The Northern Hemisphere stratosphere in the 2002/2003 winter, http://www.ozone-sec.ch.cam.ac.uk/EORCU/reports/wr0203.pdf, 2003.

Friedl-Vallon, F., Maucher, G., Kleinert, A., Lengel, A., Keim, C., Oelhaf, H., Fischer, H., Seefeldner, M., and Trieschmann, O.: Design and characterization of the balloon-borne Michelson Interferometer for Passive Atmospheric Sounding (MIPAS-B2), Appl. Opt., 43, 3335–3355, 2004.

Glatthor, N., von Clarmann, T., Fischer, H., Grabowski, U., Höpfner, M., Kellmann, S., Kiefer, M., Linden, A., Milz, M., Steck, T., Stiller, G. P., Mengistu Tsidu, G., and Wang, D.-Y.: Spaceborne ClO observations by the Michelson Interferometer for Passive Atmospheric Sounding (MIPAS) before and during the Antarctic major warming in September/October 2002, J. Geophys. Res., 109, D11307, doi:10.1029/2003JD004440, 2004.

Goldman, A., Gillis, J. R., Rinsland, C. P., and Burkholder, J. B.: Improved line parameters for the $X^2\Pi$-$X^2\Pi$ (1–0) bands of ^{35}ClO and ^{37}ClO, J. Quant. Spectrosc. Ra., 52, 357–359, 1994.

Grooß, J.-U., Günther, G., Müller, R., Konopka, P., Bausch, S., Schlager, H., Voigt, C., Volk, C. M., and Toon, G. C.: Simulation of denitrification and ozone loss for the Arctic winter 2002/2003, Atmos. Chem. Phys., 5, 1437–1448, 2005,
http://www.atmos-chem-phys.net/5/1437/2005/.

Höpfner, M., Oelhaf, H., Wetzel, G., Friedl-Vallon, F., Kleinert, A., Lengel, A., Maucher, G., Nordmeyer, H., Glatthor, N., Stiller, G., von Clarmann, T., Fischer, H., Kröger, C., and Deshler, T.: Evidence of scattering of tropospheric radiation by PSCs in mid-IR limb emission spectra: MIPAS-B observations and KOPRA simulations, Geophys. Res. Lett., 29(8), 1278, doi:10.1029/2001GL014443, 2002.

Höpfner, M., von Clarmann, T., Fischer, H., Glatthor, N., Grabowski, U., Kellmann, S., Kiefer, M.,

Linden, A., Mengistu Tsidu, G., Milz, M., Steck, T., Stiller, G. P., and Wang, D. Y.: First spaceborne observations of Antarctic stratospheric ClONO$_2$ recovery: Austral spring 2002, J. Geophys. Res., 109, D11308, doi:10.1029/2004JD004609, 2004.

Höpfner, M., von Clarmann, T., Fischer, H., Funke, B., Glatthor, N., Grabowski, U., Kellmann, S., Kiefer, M., Linden, A., Milz, M., Steck, T., Stiller, G. P., Bernath, P., Blom, C. E., Blumenstock, Th., Boone, C., Chance, K., Coffey, M. T., Friedl-Vallon, F., Griffith, D., Hannigan, J. W., Hase, F., Jones, N., Jucks, K. W., Keim, C., Kleinert, A., Kouker, W., Liu, G. Y., Mahieu, E., Mellqvist, J., Mikuteit, S., Notholt, J., Oelhaf, H., Piesch, C., Reddmann, T., Ruhnke, R., Schneider, M., Strandberg, A., Toon, G., Walker, K. A., Warneke, T., Wetzel, G., Wood, S., and Zander, R.: Validation of MIPAS ClONO$_2$ measurements, Atmos. Chem. Phys., 7, 257–281, 2007,
http://www.atmos-chem-phys.net/7/257/2007/.

IPCC (Intergovernmental Panel on Climate Change): Climate Change 2001: Synthesis Report. A Contribution of Working Groups I, II and III to the Third Assessment Report of the Integovernmental Panel on Climate Change, edited by: Watson, R. T. and the Core Writing Team, Cambridge University Press, Cambridge, UK, and New York, USA, 2001.

Jöckel, P., Sander, R., Kerkweg, A., Tost, H., and Lelieveld, J.: Technical Note: The Modular Earth Submodel System (MESSy) – a new approach towards Earth System Modeling, Atmos. Chem. Phys., 5, 433–444, 2005,
http://www.atmos-chem-phys.net/5/433/2005/.

Jöckel, P., Tost, H., Pozzer, A., Brühl, C., Buchholz, J., Ganzeveld, L., Hoor, P., Kerkweg, A., Lawrence, M. G., Sander, R., Steil, B., Stiller, G., Tanarhte, M., Taraborrelli, D., van Aardenne, J., and Lelieveld, J.: The atmospheric chemistry general circulation model ECHAM5/MESSy1: consistent simulation of ozone from the surface to the mesosphere, Atmos. Chem. Phys., 6, 5067–5104, 2006,
http://www.atmos-chem-phys.net/6/5067/2006/.

Kirner, O.: Prozessstudien der stratosphärischen Chemie und Dynamik mit Hilfe des Chemie-Klima-Modells ECHAM5/MESSy1, Dissertation, Universität Karlsruhe, 2008.

Montzka, S. A., Butler, J. H., Elkins, J. W., Thompson, T. M., Clarke, A. D., and Lock, L. T.: Present and future trends in the atmospheric burden of ozone-depleting halogens, Nature, 398, 690–694, 1999.

Nakajima, H., Sugita, T., Irie, H., Saitoh, N., Kanzawa, H., Oelhaf, H., Wetzel, G., Toon, G. C., Sen, B., Blavier, J.-F., Traub, W. A., Jucks, K., Johnson, D. G., Yokota, T., and Sasano, Y.:

Measurements of ClONO$_2$ by the Improved Limb Atmospheric Spectrometer (ILAS) in high-latitude stratosphere: New products using version 6.1 data processing algorithm, J. Geophys. Res., 111, D11S09, doi:10.1029/2005JD006441, 2006.

Nash, E. R., Newman, P. A., Rosenfield, J. E., and Schoeberl, M. R.: An objective determination of the polar vortex using Ertel's potential vorticity, J. Geophys. Res., 101, 9471–9478, 1996.

Oelhaf, H., von Clarmann, T., Fischer, H., Friedl-Vallon, F., Frietzsche, C., Linden, A., Piesch, C., Seefeldner, M., and Völker, W.: Stratospheric ClONO$_2$ and HNO$_3$ profiles inside the Arctic vortex from MIPAS-B limb emission spectra obtained during EASOE, Geophys. Res. Lett., 21, 1263–1266, 1994.

Pickett, H. M., Poynter, R. L., Cohen, E. A., Delitsky, M. L., Pearson, J. C., and Muller, H. S. P.: Submillimeter, millimeter, and microwave spectral line catalog, J. Quant. Spectrosc. Ra., 60, 883–890, 1998.

Plenge, J., Kühl, S., Vogel, B., Müller, R., Stroh, F., von Hobe, M., Flesch, R., and Rühl, E.: Bond strength of chlorine peroxide, J. Phys. Chem., 109(30), 6730–6734, 2005.

Pope, F. D., Hansen, J. C., Bayes, K. D., Friedl, R. R., and Sander, S. P.: Ultraviolet absorption spectrum of chlorine peroxide, ClOOCl, J. Phys. Chem., 111, 4322–4332, 2007.

Prinn, R. G., Huang, J., Weiss, R. F., Cunnold, D. M., Fraser, P. J., Simmonds, P. G., McCulloch, A., Harth, C., Salameh, P., O'Doherty, S., Wang, R. H. J., Porter, L., and Miller, B. R.: Evidence for substantial variations of atmospheric hydroxyl radicals in the past two decades, Science, 292, 1882–1888, 2001.

Roeckner, E., Brokopf, R., Esch, M., Giorgetta, M., Hagemann, S., Koernblueh, L., Manzini, E., Schlese, U., and Schulzweida, U.: Sensitivity of simulated climate to horizontal and vertical resolution in the ECHAM5 atmosphere model, J. Climate, 19, 3771–3791, 2006.

Rothman, L. S., Jacquemart, D., Barbe, A., et al.: The HITRAN 2004 molecular spectroscopic database, J. Quant. Spectrosc. Ra., 96, 139–204, 2005.

Sander, S. P., Friedl, R. R., Golden, D. M., Kurylo, M. J., Huie, R. E., Orkin, V. L., Moortgat, G. K., Ravishankara, A. R., Kolb, C. E., Molina, M. J., and Finlayson-Pitts, B. J.: Chemical kinetics and photochemical data for use in atmospheric studies, Evaluation no. 14, JPL Publ. 02-25, Jet Propulsion Laboratory, Pasadena, CA, 2003.

Sander, R., Kerkweg, A., Jöckel, P., and Lelieveld, J.: Technical note: The new comprehensive atmospheric chemistry module MECCA, Atmos. Chem. Phys., 5, 445–450, 2005, http://www.atmos-chem-phys.net/5/445/2005/.

Sander, S. P., Finlayson-Pitts, B. J., Friedl, R. R., Golden, D. M., Huie, R. E., Keller-Rudek, H.,

Kolb, C. E., Kurylo, M. J., Molina, M. J., Moortgat, G. K., Orkin, V. L., Ravishankara, A. R., and Wine, P. W.: Chemical kinetics and photochemical data for use in atmospheric studies, Evaluation no. 15, JPL Publ. 06-2, Jet Propulsion Laboratory, Pasadena, CA, 2006.

Santee, M. L., Manney, G. L., Waters, J. W., and Livesey, N. J.: Variations and climatology of ClO in the polar lower stratosphere from UARS Microwave Limb Sounder measurements, J. Geophys. Res., 108, 4454, doi:10.1029/2002JD003335, 2003.

Santee, M. L., MacKenzie, I. A., Manney, G. L., Chipperfield, M. P., Bernath, P. F., Walker, K. A., Boone, C. D., Froidevaux, L., Livesey, N. J., and Waters, J. W.: A study of stratospheric chlorine partitioning based on new satellite measurements and modelling, J. Geophys. Res., 113, D12307, doi:10.1029/2007JD009057, 2008.

Stiller, G. P., von Clarmann, T., Funke, B., Glatthor, N., Hase, F., Höpfner, M., and Linden, A.: Sensitivity of trace gas abundances retrievals from infrared limb emission spectra to simplifying approximations in radiative transfer modeling, J. Quant. Spectrosc. Ra., 72(2), 249–280, 2002.

Stimpfle, R. M., Wilmouth, D. M., Salawitch, R. J., and Anderson, J. G.: First measurements of ClOOCl in the stratosphere: The coupling of ClOOCl and ClO in the Arctic polar vortex, J. Geophys. Res., 109, D03301, doi:10.1029/2003JD003811, 2004.

Stowasser, M., Oelhaf, H., Ruhnke, R., Wetzel, G., Friedl-Vallon, F., Kleinert, A., Kouker, W., Lengel, A., Maucher, G., Nordmeyer, H., Reddmann, T., Trieschmann, O., von Clarmann, T., Fischer, H., and Chipperfield, M. P.: A characterization of the warm 1999 Arctic winter by observations and modeling: NO_y partitioning and dynamics, J. Geophys. Res., 107, 4376, doi:10.1029/2001JD001217, 2002.

von Clarmann, T., Fischer, H., Friedl-Vallon, F., Linden, A., Oelhaf, H., Piesch, C., Seefeldner, M., and Völker, W.: Retrieval of stratospheric O_3, HNO_3 and $ClONO_2$ profiles from 1992 MIPAS-B limb emission spectra: Method, results and error analysis, J. Geophys. Res., 98, 20495–20506, 1993.

von Clarmann, T., Wetzel, G., Oelhaf, H., Friedl-Vallon, F., Linden, A., Maucher, G., Seefeldner, M., Trieschmann, O., and Lefèvre, F.: $ClONO_2$ vertical profile and estimated mixing ratios of ClO and HOCl in the winter Arctic stratosphere from MIPAS limb emission spectra, J. Geophys. Res., 102, 16157–16168, 1997.

von Hobe, M., Grooß, J.-U., Müller, R., Hrechanyy, S., Winkler, U., and Stroh, F.: A re-evaluation of the ClO/Cl_2O_2 equilibrium constant based on stratospheric in-situ observations, Atmos. Chem. Phys., 5, 693–702, 2005,

First remote sensing measurements of ClOOCl along with ClO and ClONO₂

G. Wetzel et al.

Title Page

Abstract | Introduction

Conclusions | References

Tables | Figures

|◄ | ►|

◄ | ►

Back | Close

Full Screen / Esc

Printer-friendly Version

Interactive Discussion

http://www.atmos-chem-phys.net/5/693/2005/.

von Hobe, M., Salawitch, R. J., Canty, T., Keller-Rudek, H., Moortgat, G. K., Grooß, J.-U., Müller, R., and Stroh, F.: Understanding the kinetics of the ClO dimer cycle, Atmos. Chem. Phys., 7, 3055–3069, 2007,
http://www.atmos-chem-phys.net/7/3055/2007/.

Wagner, G. and Birk, M.: Erweiterung der spektroskopischen Datenbasis von $ClONO_2$, ClOOCl, O_3, N_2O_5 im Hinblick auf die Nutzung durch die MIPAS Instrumente, Abschlussbericht zu OFP Projekt Förderkennzeichen 07DLR05, 2001.

Wagner, G., Birk, M., Schreier, F., and Flaud, J.-M.: Spectroscopic database for ozone in the fundamental spectral regions, J. Geophys. Res., 107, 4626, doi:10.1029/2001JD000818, 2002.

Wagner, G. and Birk, M.: New infrared spectroscopic database for chlorine nitrate, J. Quant. Spectrosc. Ra., 82, 443–460, 2003.

Wetzel, G., Oelhaf, H., Ruhnke, R., Friedl-Vallon, F., Kleinert, A., Kouker, W., Maucher, G., Reddmann, T., Seefeldner, M., Stowasser, M., Trieschmann, O., von Clarmann, T., and Fischer, H.: NO_y partitioning and budget and its correlation with N_2O in the Arctic vortex and in summer mid-latitudes in 1997, J. Geophys. Res., 107, 4280, doi:10.1029/2001JD000916, 2002.

Wetzel, G., Oelhaf, H., Friedl-Vallon, F., Kleinert, A., Lengel, A., Maucher, G., Nordmeyer, H., Ruhnke, R., Nakajima, H., Sasano, Y., Sugita, T., and Yokota, T.: Intercomparison and validation of ILAS-II version 1.4 target parameters with MIPAS-B measurements, J. Geophys. Res., 111, D11S06, doi:10.1029/2005JD006287, 2006.

Wetzel, G., Sugita, T., Nakajima, H., Tanaka, T., Yokota, T., Friedl-Vallon, F., Kleinert, A., Maucher, G., and Oelhaf, H.: Technical Note: Intercomparison of ILAS-II version 2 and 1.4 trace species with MIPAS-B measurements, Atmos. Chem. Phys., 8, 1119–1126, 2008, http://www.atmos-chem-phys.net/8/1119/2008/.

Wiegele, A., Kleinert, A., Oelhaf, H., Ruhnke, R., Wetzel, G., Friedl-Vallon, F., Lengel, A., Maucher, G., Nordmeyer, H., and Fischer, H.: Spatio-temporal variations of NO_y species in the northern latitudes stratosphere measured with the balloon-borne MIPAS instrument, Atmos. Chem. Phys., 9, 1151–1163, 2009, http://www.atmos-chem-phys.net/9/1151/2009/.

WMO (World Meteorological Organization): Scientific Assessment of Ozone Depletion: 2006, Global Ozone Research and Monitoring Project – Report No. 50, 572 pp., Geneva, Switzerland, 2007.

First remote sensing measurements of ClOOCl along with ClO and ClONO$_2$

G. Wetzel et al.

First remote sensing measurements of ClOOCl along with ClO and ClONO2

G. Wetzel et al.

Table 1. Set-up for MIPAS-B sensitivity studies and retrievals. Results are given for different species in corresponding spectral windows.

Species	Band (µm)	Spectral range (cm^{-1})	Interfering species	Signal to noise ratio at 18 km $\Delta m=20\%$	$\Delta m=-100\%$	D.o.f.	Alt. reso. (km)
ClO	11.8	821.0–841.5	O_3, CO_2, NO_2, HNO_3, H_2O, $ClONO_2$, CFC-22, CFC-11	3.0^c, 4.4^d (day) 0.4^c, 0.5^d (night)	15^c, 22^d (day) 1.9^c, 2.5^d (night)	4.5	3–7
ClOOCl	13.3	721.0–788.0^a 755.0–788.0^b	O_3, CO_2, HNO_3, COF_2, HCN, $ClONO_2$, N_2O_5	0.4^c, 4.4^d (night)	2.0^c, 22^d (night)	4.0	3–7
ClONO$_2$	12.8	779.7–780.7	O_3, CO_2, HNO_3	51^c, 88^d	419^c, 548^d	11–12	1.5–3

[a] used for sensitivity studies;
[b] used for retrieval calculations.
[c] Signal to noise ratio (SNR_i) refers to the maximum signal of the target molecule spectral feature at one grid point in the spectral window assuming a measurement time of 1.5 min (10 averaged spectra). Δm corresponds to changing the signal by varying the mass m of the target molecule by 20% and −100%, respectively.
[d] Using a number of independent grid points N in the retrieval improves the signal to noise ratio (SNR_N) by $N^{0.5}$. Degrees of freedom (D.o.f.) are calculated from the main diagonal elements of the averaging kernel and are given together with the corresponding altitude resolution (Alt. reso.).
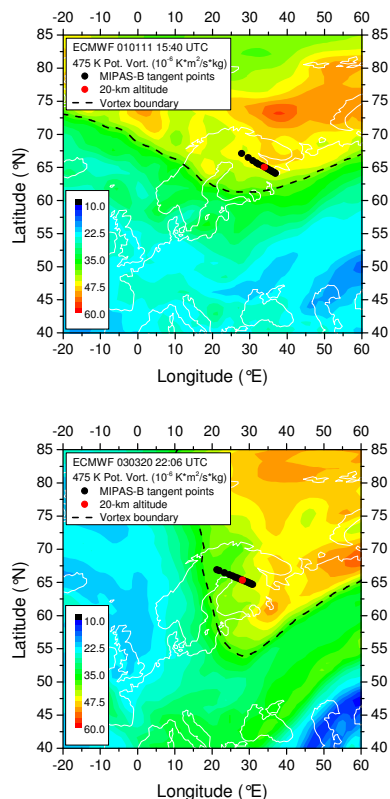
Fig. 1. Potential vorticity (PV) fields from European Centre for Medium-Range Weather Forecasts (ECMWF) analyses on 11 January 2001 (top) and 20 March 2003 (bottom), interpolated to the MIPAS-B observation times, at the 475 K potential temperature surface (about 20 km altitude). MIPAS-B tangent points are plotted as black solid circles (20-km altitude in red colour). Vortex boundaries, representing the strongest PV gradient (Nash et al., 1996) are shown as dashed lines.

Title Page

Abstract | Introduction

Conclusions | References

Tables | Figures

|◄ | ►|

◄ | ►

Back | Close

Full Screen / Esc
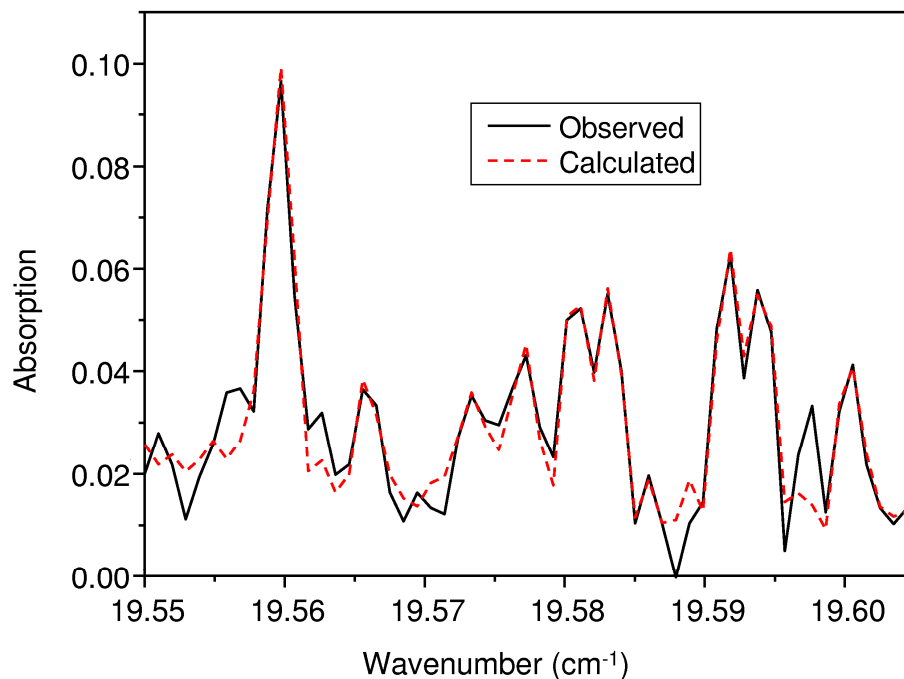
Fig. 2. Microwindow showing observed and calculated individual rotational transitions of ClOOCl. The contaminants (Cl_2O_3, ClO, HOCl and OClO) were also modelled, e.g. the line at 19.592 cm^{-1} is OClO. The amounts of the contaminants were well below 1%. However, their line strengths are much larger when compared to ClOOCl. Spectra of the precursor Cl_2O were also measured, scaled and divided before fitting to remove Cl_2O lines.
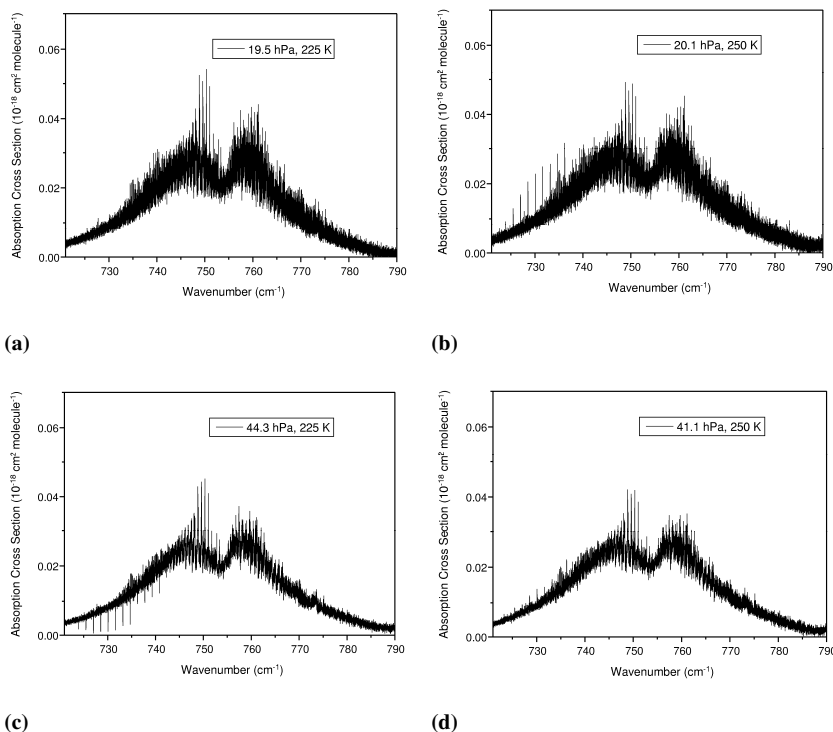
Fig. 3. Absorption cross sections of the ClOOCl ν_1 band at different total pressures and temperatures **(a–d)**. The band structure is dominated by partly resolved P- and R-branches. A high resolution structure is visible and, as expected, stronger in the low pressure case. The technical chlorine unfortunately contained CO_2 yielding huge lines. The CO_2 was subtracted out but some residual lines remain visible in the lower wavenumber part of the spectra at 20.1 hPa/250 K and 44.3 hPa/225 K (negative CO_2 peaks). The peak-to-peak noise level of the 40/20 hPa measurements is $0.01/0.02 \times 10^{-18}\,cm^2\,molecule^{-1}$. Temperature dependence is rather small.

Full Screen / Esc

Printer-friendly Version

Interactive Discussion
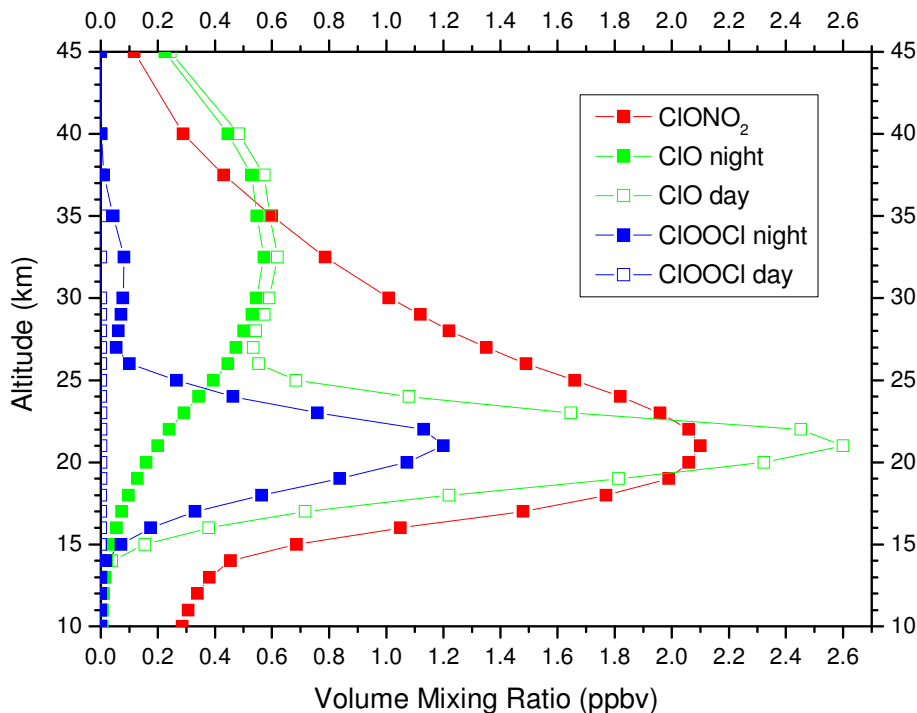
Fig. 4. Arctic winter profiles of chlorine species used for the radiance sensitivity calculations. ClO (day) and ClOOCl (night) profiles correspond to activated chlorine conditions; ClONO₂ mixing ratios represent deactivated air masses.
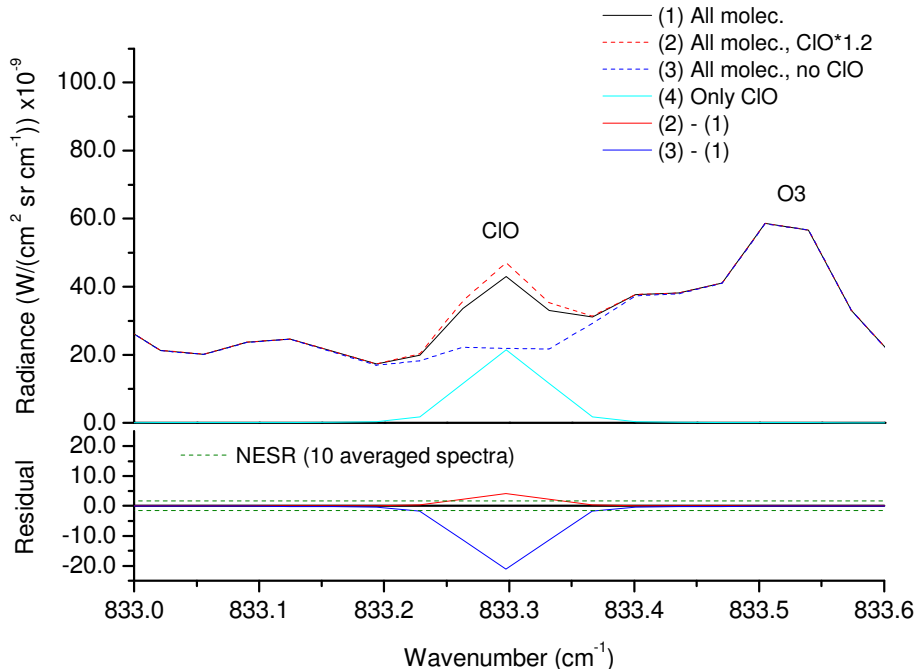
Fig. 5. Radiance simulations around a well-separated ClO signature from 833.0–833.6 cm⁻¹ for activated polar winter day conditions at a tangent altitude of 18 km. The figure shows a calculation taking into account all emitting molecules (black solid line); simulations with enhanced ClO ($\Delta m = +20\%$; red dotted line), without ClO ($\Delta m = -100\%$; blue dotted line), and with ClO alone (cyan solid line). Differences are plotted in the bottom part of the figure (red and blue solid lines). The typical spectral noise band (NESR) of the MIPAS-B instrument is also displayed (green dotted lines).
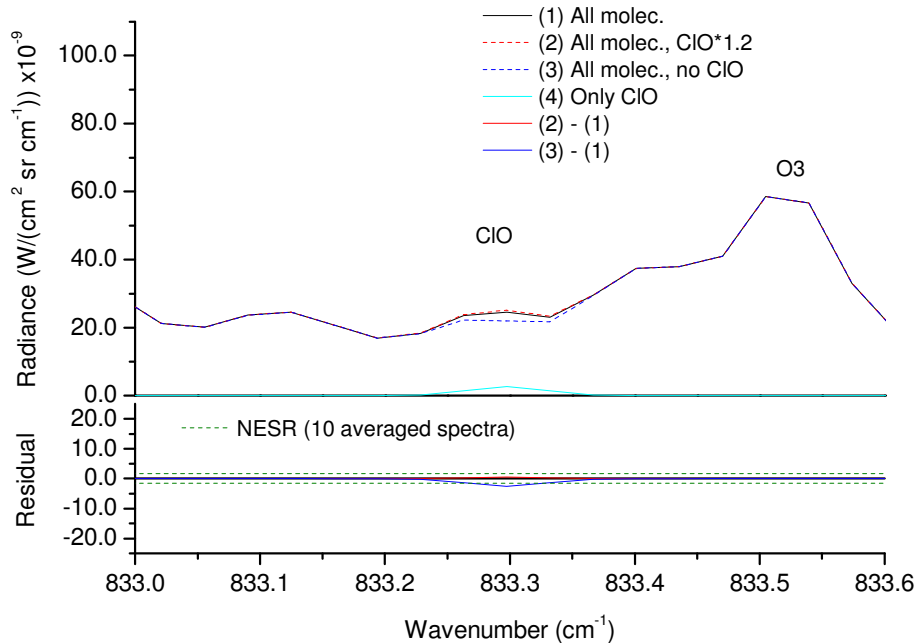
Fig. 6. Same as Fig. 5 but for polar winter night conditions.
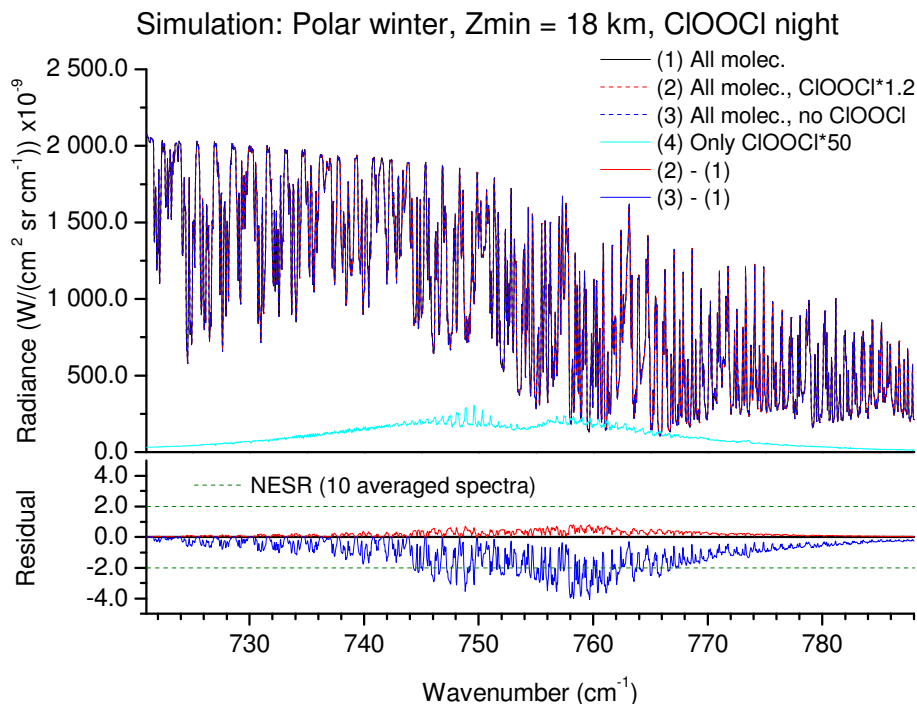
Fig. 7. Simulation for ClOOCl in polar night in chlorine-activated conditions. Broadband radiance calculations for the 18-km tangent altitude in the spectral window from 721 to 788 cm^{-1} comprising the mid-infrared ClOOCl band centred near 753 cm^{-1}. Notation as per Fig. 5. Please note, that in simulation (4) ClOOCl is scaled by a factor of 50 for better clarity.
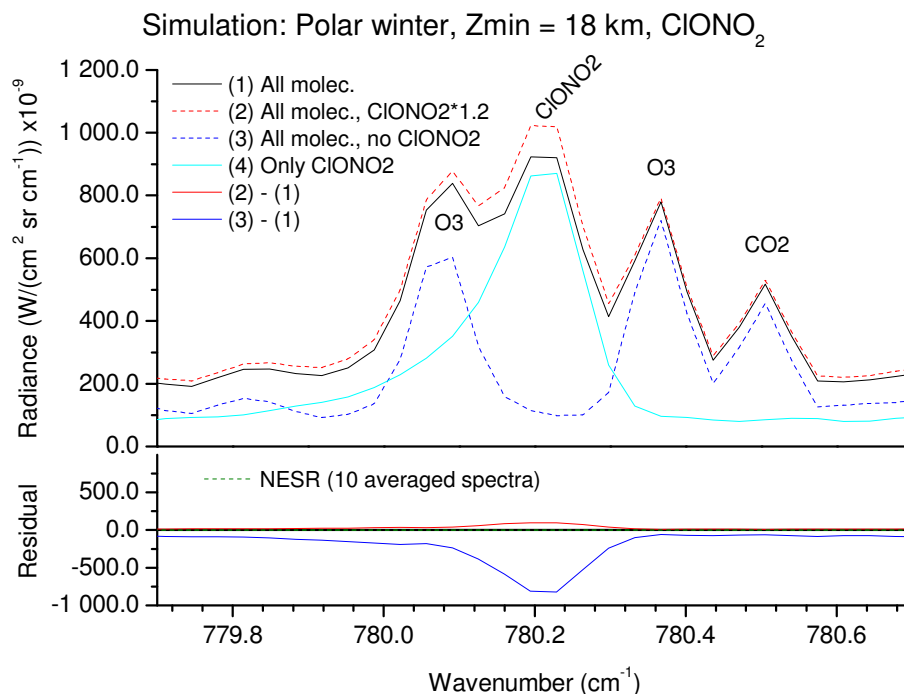
Fig. 8. Radiance simulations in the spectral region of the ClONO₂ ν_4 Q-branch between 779.7 and 780.7 cm^{-1} for a tangent altitude of 18 km (Arctic spring, deactivated chlorine). Notation as per Fig. 5. Calculated signal-to-noise ratios for the centre of the ClONO₂ Q-branch are about 50 for a Δm of 20%. The noise level (NESR) of the MIPAS-B instrument is only about 2×10^{-9} W/(cm² sr cm^{-1}) in this spectral region (for an integration time of 1.5 min).
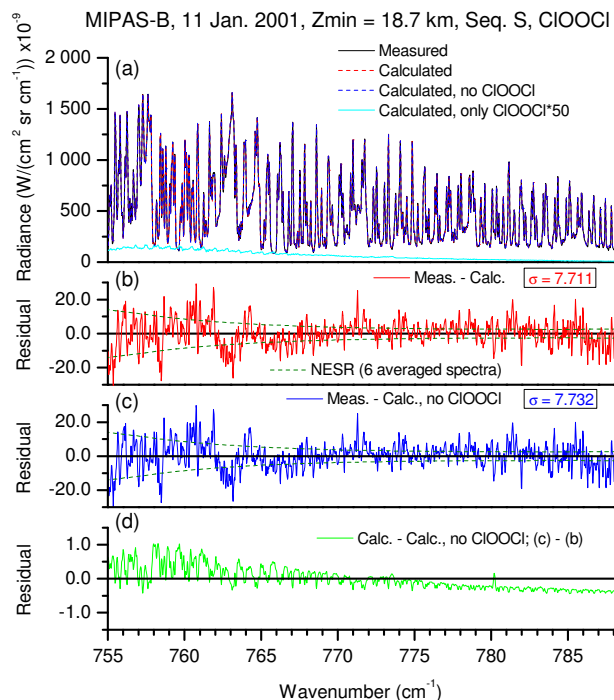
Fig. 9. Best fit of measured MIPAS-B spectra in the R-branch region of the ClOOCl 13.3 μm band corresponding to a tangent altitude of 18.7 km. **(a)** Measured spectrum (black solid line); calculated spectrum (red dotted line); calculated spectrum without ClOOCl (blue dotted line); calculated spectrum with only (retrieved) ClOOCl emissions, scaled by a factor of 50 (solid cyan line). **(b)** Residual spectrum "measured – calculated" (red solid line); NESR (dark green dotted line) is shown together with root of mean squares (σ). **(c)** Residual spectrum "measured – calculated without ClOOCl" (blue solid line) together with NESR and σ. **(d)** Residual spectrum "calculated – calculated without ClOOCl" (green solid line), corresponding to the difference (c–b).

Title Page

Abstract   Introduction

Conclusions   References

Tables   Figures

◄   ►|

◄   ►

Back   Close

Full Screen / Esc

Printer-friendly Version

Interactive Discussion
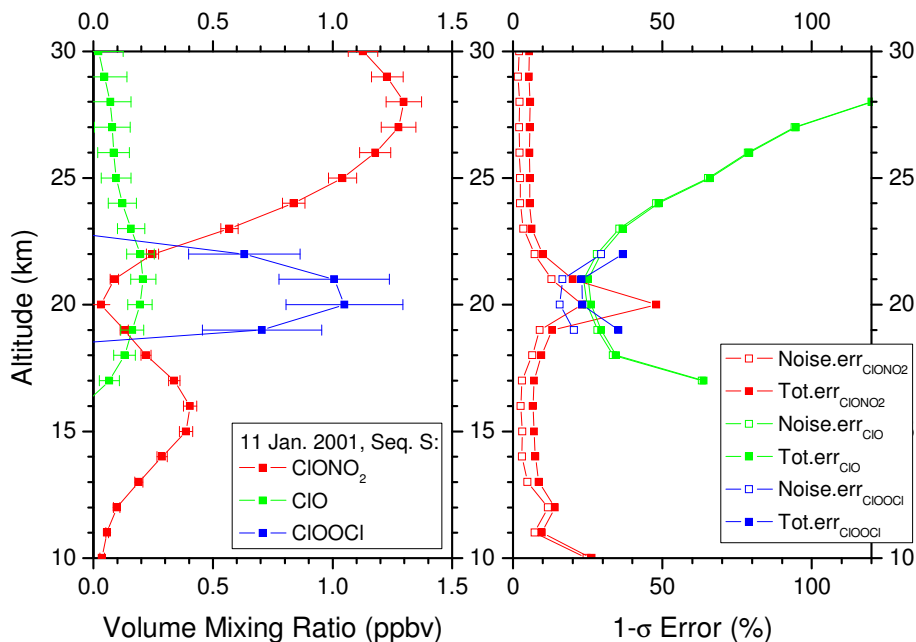
Fig. 10. Retrieved results in chlorine-activated conditions (night-time). Vertical profiles of the species ClONO$_2$, ClO, and ClOOCl, as measured by MIPAS-B on 11 January 2001 above Kiruna with absolute total errors (left) and relative random (noise and covariance effects of the fitted parameters) and total errors (right). While random errors are dominant for nighttime ClO, systematic error sources are also important for the ClOOCl analysis.
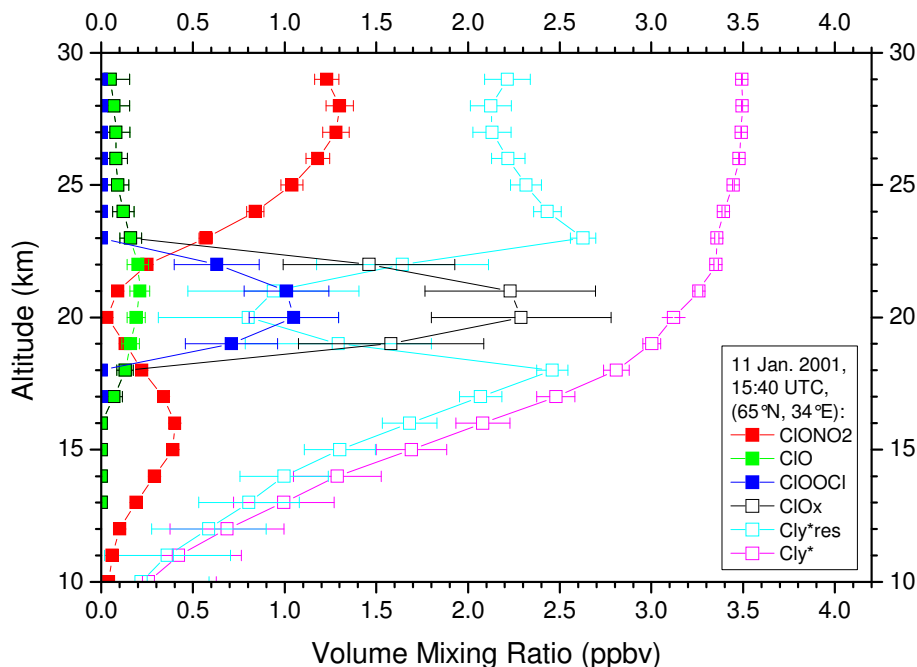
Fig. 11. Chlorine species as measured by MIPAS-B on 11 January 2001 inside the polar vortex above northern Scandinavia. Besides ClONO$_2$, ClO, ClOOCl, and ClO$_x$, Cl$^*_{yres}$ (mainly HCl) and total inorganic chlorine Cl$^*_y$ (consisting of ClO$_x$, ClONO$_2$, and Cl$^*_{yres}$), are plotted, too. Cl$^*_y$ is calculated from MIPAS-B N$_2$O via a N$_2$O-Cl$_y$ correlation deduced from in-situ observations of Arctic balloon flights between 2000 and 2003. Cl$^*_{yres}$ has been derived from the difference of Cl$^*_y$ minus ClONO$_2$ and ClO$_x$. A layer of activated chlorine (ClO$_x$~2.3 ppbv, ClONO$_2$<0.1 ppbv) is visible in the measurements around 20 km.
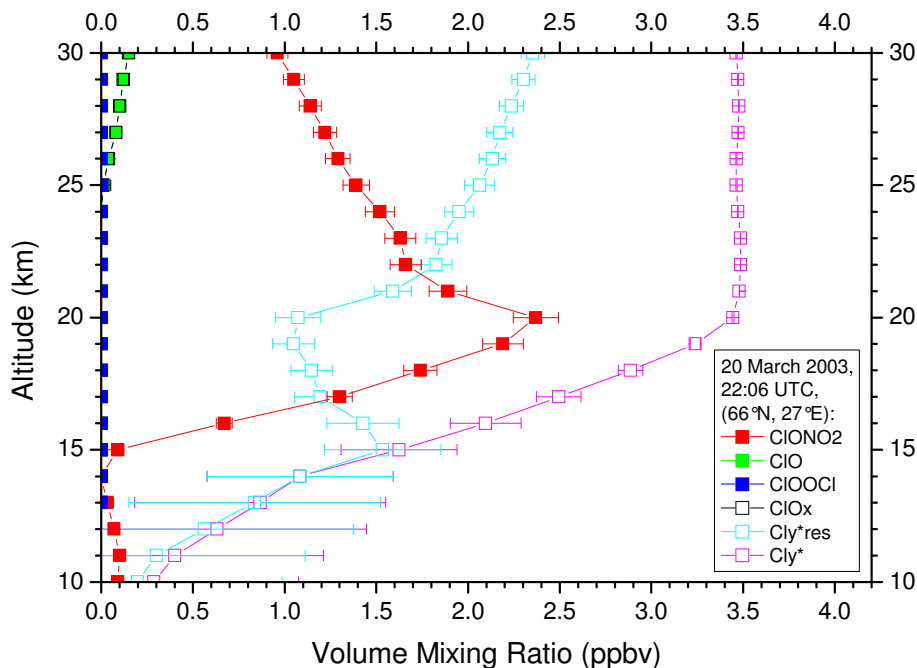
Fig. 12. Chlorine species as measured by MIPAS-B on 20 March 2003 inside the Arctic vortex. Notation as per Fig. 11. Deactivation of active chlorine is expressed by high ClONO$_2$ values around 20 km.
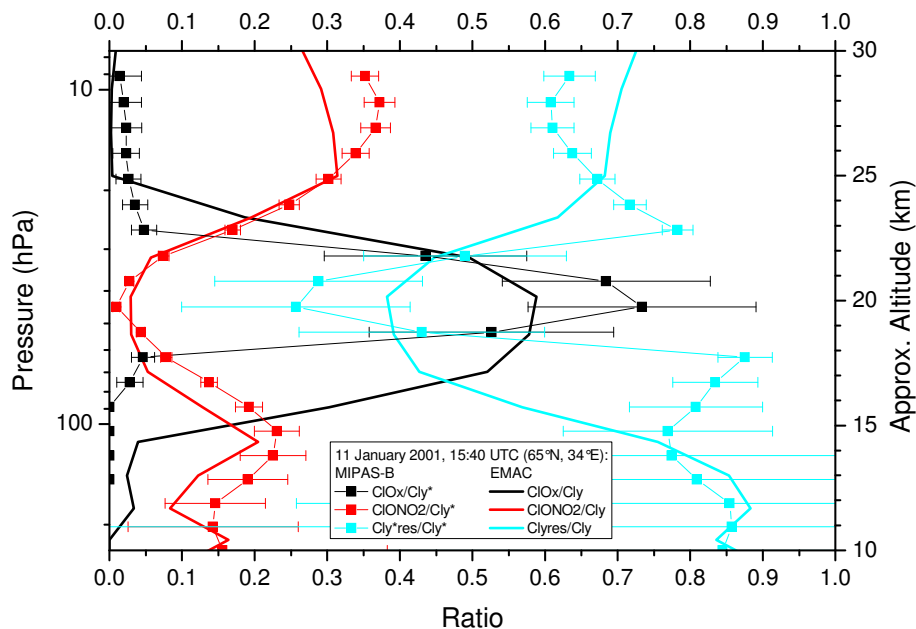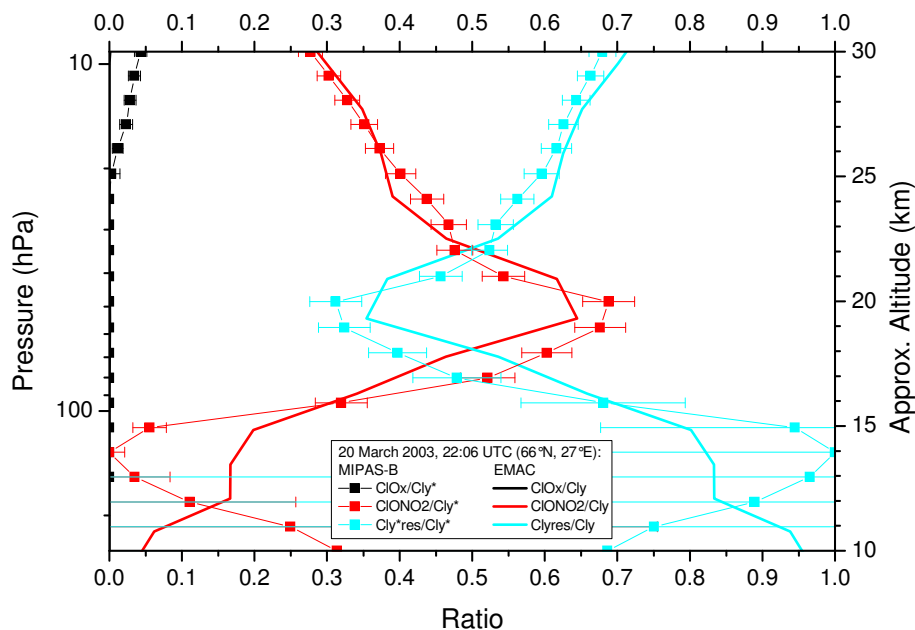
Fig. 13. Ratios of active chlorine to total inorganic chlorine as measured by MIPAS-B on 11 January 2001 in comparison to simulations of the chemistry climate model EMAC.

Fig. 14. Same as Fig. 13 but for 20 March 2003.

[ACPD](#)

9, 20103–20143, 2009

First remote sensing measurements of ClOOCl along with ClO and ClONO$_2$

G. Wetzel et al.

Title Page

Abstract | Introduction

Conclusions | References

Tables | Figures

|◄ | ►|

◄ | ►

Back | Close

Full Screen / Esc
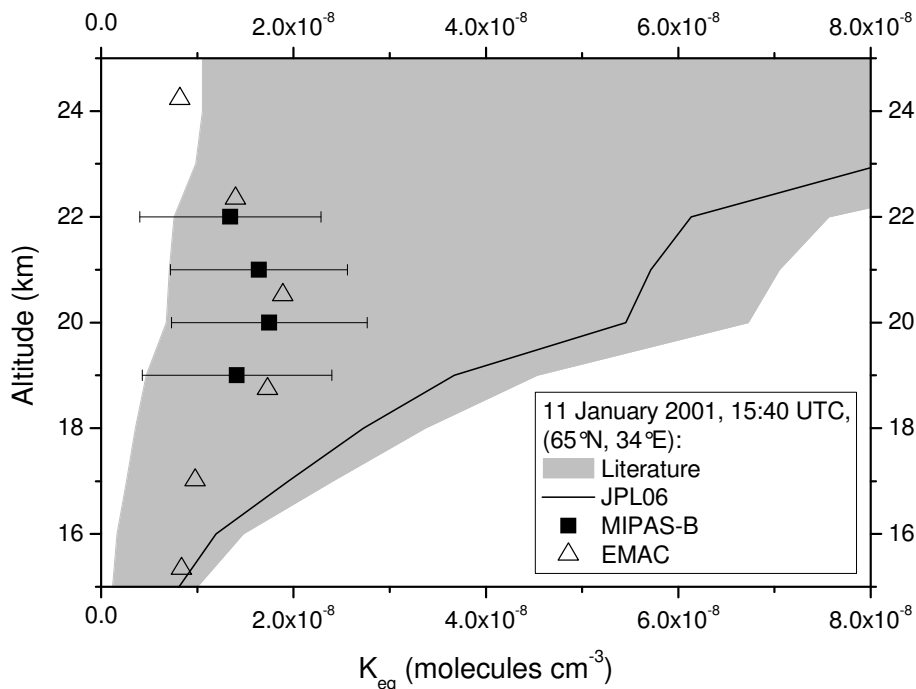
Printer-friendly Version

Interactive Discussion

Fig. 15. ClO/ClOOCl equilibrium constant K_{eq} calculated via Eq. (1) for MIPAS-B observations and simulations of the chemical model EMAC. JPL06 (Sander et al., 2006) and further data from literature are calculated using the JPL format $K = A \times \exp(B/T)$ with corresponding coefficients A and B (see, von Hobe et al., 2007 and references therein) and temperature T as measured by MIPAS-B.